Magazine of Concrete Research
Volume 67 Issue 20

Seismic response modification factors of reinforced concrete staggered wall structures
Lee and Kim

Magazine of Concrete Research, 2015, **67**(20), 1070–1083
http://dx.doi.org/10.1680/macr.14.00036
Paper 1400036
Received 29/01/2014; revised 25/12/2014; accepted 10/04/2015
Published online ahead of print 21/05/2015

ice
Institution of Civil Engineers
publishing

Seismic response modification factors of reinforced concrete staggered wall structures

Joonho Lee
Postdoctoral researcher, Department of Civil and Architectural Engineering, Sungkyunkwan University, Suwon, Korea

Jinkoo Kim
Professor, Department of Civil and Architectural Engineering, Sungkyunkwan University, Suwon, Korea

This study investigated the response modification factor for reinforced concrete staggered wall structures based on the approach of the Federal Emergency Management Agency (Fema P695). In this study, 24 model structures, categorised into 14 performance groups, were designed as per recommendations of the American Society of Civil Engineers (ASCE 7-10) using two different response modification factors. Incremental dynamic analyses were carried out using 44 earthquake records, and the results were used to obtain fragility curves. The results showed that model structures designed with a response modification factor (R) of 3 satisfied the acceptance criteria specified in Fema P695. However, the model structures designed with $R = 6$ and categorised as seismic design category D_{max} failed to satisfy the acceptance criteria. Based on this observation, response modification factors of 4 to 5 are recommended for staggered wall system structures.

Notation

A_{cv}	gross area of concrete section
C	structural capacity
C_0	coefficient relating fundamental mode displacement to roof displacement
$\hat{C}$	median structural capacity
C_s	seismic response coefficient
D	structural demand
E	elastic modulus
F_R	residual stress
F_u	ultimate stress
F_y	yield stress
f'_c	ultimate strength of concrete
f_y	yield strength of rebars
G	shear modulus
h_w	height of wall
K_o	initial stiffness
K_h	post-yield stiffness
l_w	length of wall
R	response modification factor
S_{MS}	short-period spectral acceleration of MCE earthquakes
S_{M1}	1 s-period spectral acceleration of MCE earthquakes
S_a	spectral acceleration
$\hat{S}_{CT}$	median collapse intensity
S_{D1}	seismic coefficient for 1 s period
S_{DS}	seismic coefficient for short period
S_{MT}	maximum considered earthquake intensity
T_1	fundamental period of the archetype model
T_s	transition period
V	design base shear
V_m	maximum base shear
V_y	shear yield strength of staggered walls
W	weight of model structure
β_c	system collapse uncertainty
γ_y	shear yield strain
γ_u	ultimate shear strain
δ_{eff}	effective roof drift displacement
δ_u	ultimate roof drift displacement
λ	modification factor for lightweight concrete
μ_T	period-based ductility
ρ_t	ratio of area of transverse reinforcement to gross concrete area perpendicular to that reinforcement
τ_y	shear yield stress
Ω	over-strength factor

Introduction

The design of more sustainable structures has become an important issue in the construction industry. In Korea, traditionally most residential buildings were designed with many shear walls that act as partition walls as well as lateral and gravity load resisting systems. Even though such a practice resulted in the economic use of structural materials and easy construction of residential buildings, these buildings are now not favoured, mainly because the traditional plan layouts that divide a building into many small spaces by vertical shear walls fail to meet the demand of people who prefer large open spaces. To enhance the possibility of reshaping the plan layout of residential buildings, the Korean government provides various incentives for apartment buildings designed with increased spatial flexibility. In this regard, apartment buildings with vertical walls placed at alternate levels have drawn the attention of architects and structural engineers, due to their enhanced spatial flexibility while maintaining the economy and constructability of shear wall structures. Structural systems such as these have already been widely applied in steel residential buildings and are typically called staggered truss systems. Even though they have not yet been realised in reinforced concrete (RC) buildings, the idea was suggested many years ago.

Fintel (1968) proposed a staggered system for RC buildings, called the staggered wall–beam structure, in which staggered walls with attached slabs resist gravity as well as lateral loads as H-shaped storey-high deep beams. Fintel conducted experiments using half-scale staggered wall structures subjected to gravity load. He noted that the staggered wall systems were very competitive compared with conventional forms of construction, and in many cases would actually be more economical. Mee *et al.* (1975) investigated the structural performance of staggered wall systems subjected to dynamic load by carrying out shaking table tests of 1/15 scaled models. Kim and Jun (2011) evaluated the seismic performance of partially staggered wall apartment buildings using non-linear static and dynamic analysis. More recently, Lee and Kim (2013) investigated the seismic performance of staggered wall structures with a middle corridor, and Kim and Lee (2014) proposed a formula for the fundamental natural period of staggered wall structures.

The current study investigated the response modification factor (R factor) of staggered wall structures based on the procedure presented in the Federal Emergency Management Agency's quantification of building seismic performance factors (Fema P695) (Fema, 2009). A total of 24 model structures were prepared: 8 staggered wall structures were designed with $R = 3$ and the other 16 structures with $R = 6$. The factor $R = 3$ was chosen as the lower bound based on the observation that it is generally applied for structures not defined as one of the seismic force resisting systems in seismic design codes. The upper bound of $R = 6$ was selected because it is the highest value specified for RC shear wall structures in ASCE 7-10: Minimum design loads for buildings and other structures (ASCE, 2010).The validity of the R factors used for the seismic design of the model structures was investigated by comparing the seismic failure probability of the model structures with the limit states given in Fema P695 (Fema, 2009).

Design of model structures for analysis

Configuration of staggered wall–beam system

In staggered wall systems, the storey-high RC walls that span the width of the building are located along the short direction in a staggered pattern. The floor system spans from the top of one staggered wall to the bottom of the adjacent wall, serving as a diaphragm, and the staggered walls are designed as storey-high deep beams. The staggered walls, with attached slabs, resist gravity as well as lateral loads as H-shaped deep beams. The horizontal shear force from the staggered walls above flows to the columns and staggered walls below through the floor diaphragm. With RC walls located at alternate floors, flexibility in spatial planning can be achieved compared to conventional structures with vertically continuous shear walls. Columns and beams are located along the longitudinal perimeter of the structures, providing a full width of column-free area within the structure. Along the longitudinal direction, the column–beam combination resists lateral load as a moment resisting frame.

Structural design of model structures

Staggered truss or staggered wall–beam systems have not been considered as one of the basic seismic force resisting systems in most design codes. Fema 450 (Fema, 2003) requires that lateral systems that are not listed as a basic seismic force resisting system shall be permitted if analytical and test data are submitted to demonstrate the lateral force resistance and energy dissipation capacity. In this regard, Fema P695 (Fema, 2009) provides a rational basis for determining building seismic performance factors that will result in equivalent seismic safety against collapse for buildings with different seismic force resisting systems. The methodology determines the response modification coefficient, also called the R factor, using a sufficient number of non-linear models of seismic force resisting system archetypes to capture the variability of the seismic performance characteristics of the system of interest. Archetype design assumes a trial value of R to determine the seismic response coefficient, C_s. The structural system archetypes need to be representative of the variations that would be permitted in actual structures. Archetypes are designed to have different characteristics such as seismic design category (SDC), building height and fundamental period, bay sizes, wall lengths and so on. Structural system archetypes are assembled into performance groups, which reflect changes in behaviour. The collapse safety of the proposed system

Gravity load	
Dead load: kN/m^2	7
Live load: kN/m^2	2·5
Wind load	
Exposure category	B
Basic wind speed: m/s	30
Importance factor	1·0
Gust effect factor	2·2
Seismic load	
Site class	S_d
S_{DS}	1·0 (D_{max}), 0·5(C_{max})
S_{D1}	0·6 (D_{max}), 0·2(C_{max})
Importance factor	1·0
Response modification coefficient, R	6·0, 3·0

Table 1. Design parameters for analysis of model structures

is then evaluated for each performance group. Fema P695 (Fema, 2009) requires statistical evaluation of short-period archetypes separately from long-period archetypes, and distinguishes between them on the basis of the transition period T_s, defined as

1. $$T_s = \frac{S_{D1}}{S_{DS}} = \frac{S_{M1}}{S_{MS}}$$

	Steel	Concrete
Design factor	1·25	1·25
E: kN/cm^2	—	2696·4
Ultimate strength: MPa	$f_y = 400$	$f'_c = 24$
	Expected $f_y = 500$	Expected $f'_c = 30$

Table 2. Nominal and expected strengths of structural materials

In this study, the model structures were designed as per ACI 318-14 (ACI, 2014) using the seismic loads specified in the International Building Code (ICC, 2009). The dead and live loads were 7·0 kN/m^2 and 2·5 kN/m^2 respectively. The model structures were designed into two different groups with SDCs of D_{max} and C_{max}. The seismic coefficients S_{DS} and S_{D1} of the structures in each category are presented in Table 1. Table 2 shows the nominal and expected strengths of the steel and concrete materials used in the design and analysis of the model structures. To meet the Fema P-695 (Fema, 2009) requirements, the model structures were categorised into many performance groups. Tables 3 and 4 show

Performance group	Model	Wall length: m	SDC	Period domain	Number of storeys	Period: s	Transient period: s
PG1	R3 6D8	6	D_{max}	Short	8	0·345	0·6
PG1	R3 6D12	6	D_{max}	Short	12	0·584	0·6
PG2	R3 6C8	6	C_{max}	Short	8	0·381	0·4
PG3	R3 6C12	6	C_{max}	Long	12	0·640	0·4
PG4	R3 9D8	9	D_{max}	Short	8	0·249	0·6
PG4	R3 9D12	9	D_{max}	Short	12	0·431	0·6
PG5	R3 9C8	9	C_{max}	Short	8	0·266	0·4
PG6	R3 9C12	9	C_{max}	Long	12	0·470	0·4

Table 3. Performance groups of model structures designed with response modification factor of 3

Performance group	Model	Wall length: m	SDC	Period domain	Number of storeys	Period: s	Transient period: s
PG1	R6 6D4	6	D_{max}	Short	4	0·143	0·6
PG1	R6 6D8	6	D_{max}	Short	8	0·363	0·6
PG2	R6 6D12	6	D_{max}	Long	12	0·623	0·6
PG2	R6 6D16	6	D_{max}	Long	16	0·983	0·6
PG3	R6 6C4	6	C_{max}	Short	4	0·146	0·4
PG3	R6 6C8	6	C_{max}	Short	8	0·395	0·4
PG4	R6 6C12	6	C_{max}	Long	12	0·676	0·4
PG4	R6 6C16	6	C_{max}	Long	16	1·015	0·4
PG5	R6 9D4	6	D_{max}	Short	4	0·111	0·6
PG5	R6 9D8	9	D_{max}	Short	8	0·262	0·6
PG5	R6 9D12	9	D_{max}	Short	12	0·459	0·6
PG6	R6 9D16	9	D_{max}	Long	16	0·699	0·6
PG7	R6 9C4	9	C_{max}	Short	4	0·133	0·4
PG7	R6 9C8	9	C_{max}	Short	8	0·281	0·4
PG8	R6 9C12	9	C_{max}	Long	12	0·492	0·4
PG8	R6 9C16	9	C_{max}	Long	16	0·769	0·4

Table 4. Performance groups of model structures designed with response modification factor of 6

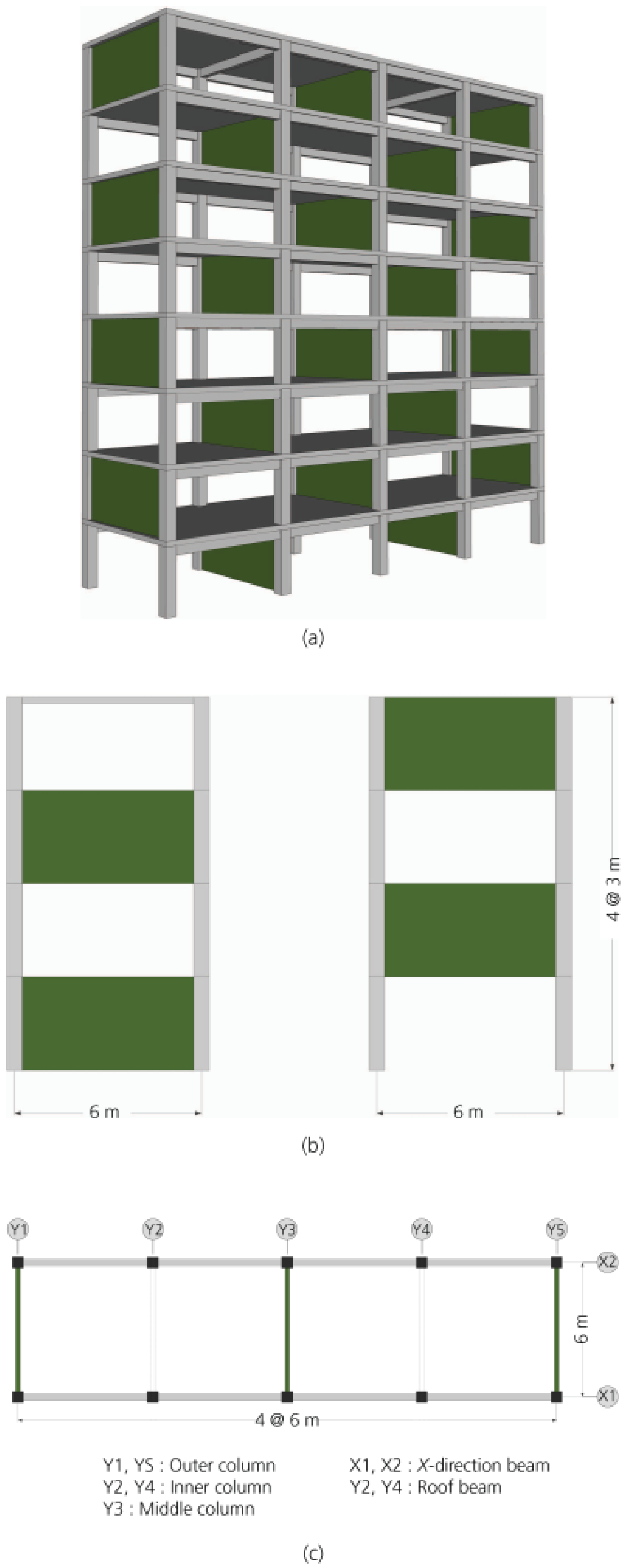

Figure 1. Configuration of the model structure with 6 m staggered walls: (a) 3D view of a staggered wall–beam system; (b) elevation view (c) structural plan

the model structures designed with R factors of 3 and 6 respectively, and the performance groups they belong to. The natural and transient periods of the model structures are also presented in the tables. For variation of basic structural configuration, the model structures were divided into two groups depending on the length of the staggered walls. To consider the effect of the natural period, the model structures designed with $R = 3$ were divided into 8-storey and 12-storey structures, and those designed with $R = 6$ were divided into structures with 4, 8, 12 and 16 storeys. The distinction between short and long period domains was made based on the transition period computed using Equation 1.

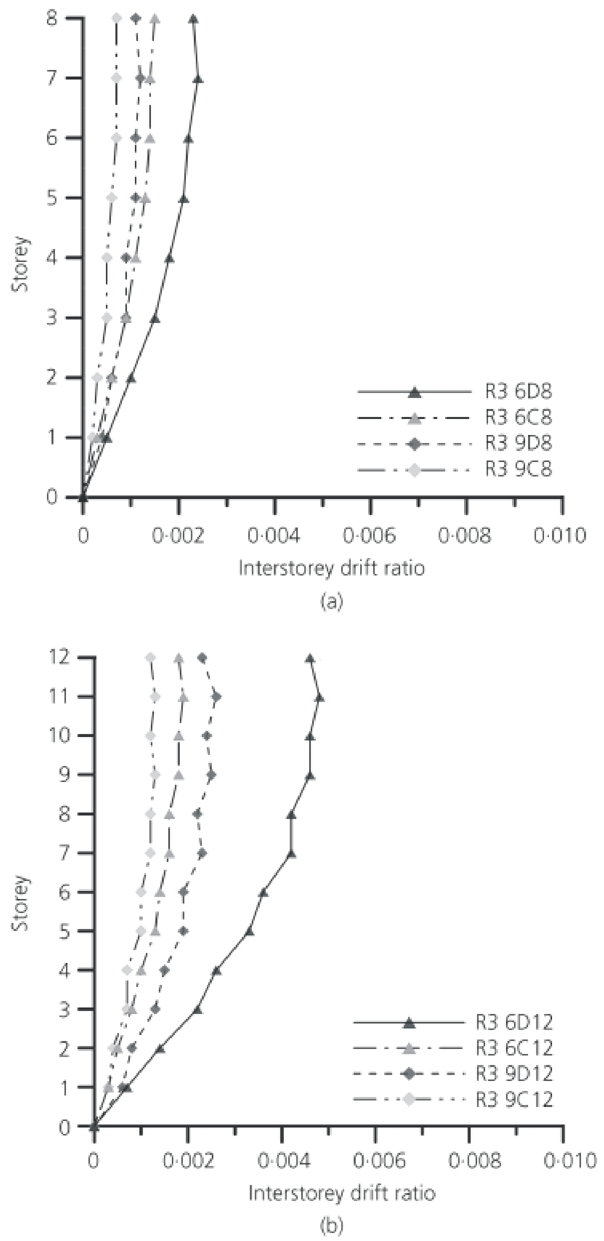

Figure 2. Interstorey drift of the model structures designed with $R = 3$: (a) 8-storey; (b) 12-storey

Figure 1 shows the configuration of the model structure with 6 m staggered walls along the transverse direction, and with two moment frames along the longitudinal direction. The thickness of the staggered walls was 200 mm in all storeys. The staggered walls act like deep beams with the depth of a storey in height, and were reinforced with vertical and horizontal rebars of 13 mm diameter at 400 mm intervals. The structural members were designed so that the ratio of the member force to the design strength was maintained at 0·8–0·9. In every column, 10 mm tie bars were placed at intervals of 200 mm. The thickness of the floor slabs was 210 mm, which is the minimum thickness required for wall-type apartment buildings in Korea to prevent the transmission of excessive noise and vibration through the floors. Figure 2 shows the interstorey drifts of the model structures designed with $R = 3$ subjected to the design seismic loads. It can be observed that the interstorey drift generally increased as storey height increased, which implies that the staggered wall structures behave more like structures with shear walls than moment resisting frames. It can also be seen that the maximum interstorey drifts of the model structures were significantly smaller than the limit state of 2% of storey height as specified in ASCE 7-10 (ASCE, 2010). Based on the small interstorey drift and the observation that the natural periods of the staggered wall model structures shown in Table 3 were generally shorter than half of those of typical moment resisting frames of similar size, it can be concluded that the staggered wall structures are stiff compared with typical moment resisting frames. The nominal strengths of the concrete and rebars were 24 MPa and 400 MPa respectively, and the expected strengths of the rebars and concrete were assumed to be 1·25 times the nominal strength (Peer, 2011).

Modelling for non-linear analysis

The Fema P695 methodology requires detailed modelling of the non-linear behaviour of archetypes sufficient to capture collapse failure modes (Fema, 2009). The stress–strain relationships of vertical and horizontal bending were defined as tri-linear lines, as shown in Figure 3(a) and based on the material model of Paulay and Priestley (1992) without a confinement effect. In the model, the ultimate strength and yield strength of concrete were 24 MPa and 14 MPa respectively, and the residual strength was defined as 20% of the ultimate strength. The strain at the ultimate strength was 0·002 and the ultimate strain was defined as 0·004. The reinforcing steel was modelled with bi-linear lines, as shown in Figure 3(b). The staggered walls were modelled using the general wall fibre elements provided in Perform-3D (CSI, 2006). The shear yield strength of the staggered walls was computed based on ACI 318-14 (ACI, 2014) as

$$V_y = A_{cv}[\alpha_c \lambda (f'_c)^{1/2} + \rho_t f_y] \quad (2)$$

where the coefficient α_c varies linearly between 0·25 and 0·17 for h_w/l_w between 1·5 and 2·0; $\alpha_c = 0{\cdot}25$ for $h_w/l_w \leqslant 1{\cdot}5$ and $\alpha_c = 0{\cdot}17$ for $h_w/l_w \geqslant 2{\cdot}0$ (h_w is the height of the entire wall from base to top or height of the segment of wall considered, and l_w is the length of the entire wall or the length of segment of wall considered in the direction of shear force). A_{cv} is the gross area of concrete section bounded by the web thickness and the length of section in the direction of shear force considered, ρ_t is the ratio of area of transverse reinforcement to gross concrete area perpendicular to that reinforcement, and $\lambda$is a modification factor reflecting the reduced mechanical properties of lightweight concrete ($\lambda = 1{\cdot}0$ for normal weight concrete).

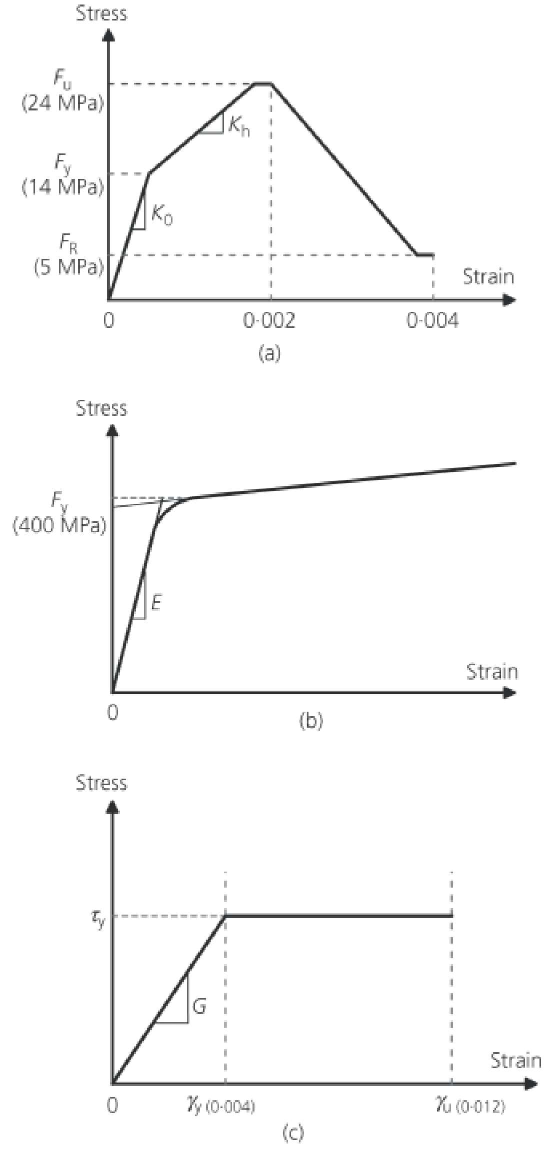

Figure 3. Non-linear stress–strain relationship of staggered walls: (a) axial stress–strain relationship of concrete; (b) axial stress–strain relationship of steel; (c) shear deformation of general wall element

The shear stress–strain relationship of the staggered wall was modelled by bi-linear lines with yield and ultimate strains of 0·004 and 0·012 respectively, as shown in Figure 3(c). The

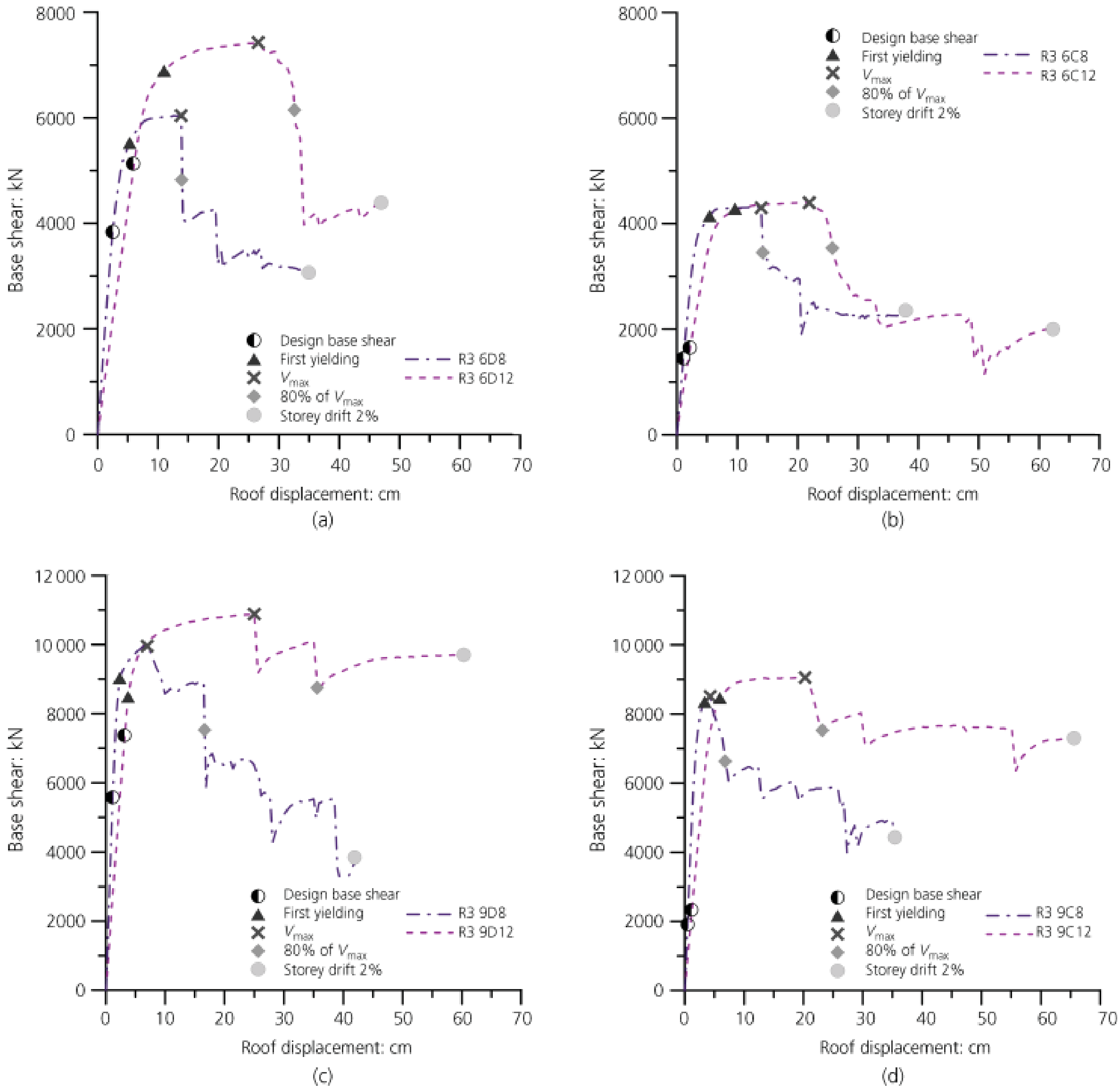

Figure 4. Non-linear static pushover analysis results of the structures designed with $R = 3$: (a) PG1; (b) PG2, PG3; (c) PG4; (d) PG5, PG6

staggered walls were modelled using fibre elements with 0·32% reinforcement in each element.

Evaluation of response modification factor using the Fema P695 procedure

Overall procedure

Non-linear static and dynamic analyses are generally required to evaluate the response modification factor of a structure based on Fema P695 (Fema, 2009). Ground motions are scaled to represent a range of earthquake intensities up to collapse-level ground motions. Individual records are normalised by their respective peak ground velocities to remove unwarranted variability between records due to inherent differences in event magnitude, distance to source, source type and site conditions. A non-linear static (pushover) analysis is performed to check the non-linear behaviour of the structure, to verify that all elements have not yielded at the point that a collapse mechanism develops in the structure. The ductility capacity is determined from the results of pushover analysis, and the spectral shape factor (SSF) is determined based on the ductility capacity and the fundamental period. A non-linear incremental dynamic analysis of a structure is performed for each scaled record of the record set. If less than one-half of the records cause collapse, then the trial design meets the given

Model	V: kN	V_{max}: kN	Ω	C_0	W: kN	T_1: s	δ_{eff}: cm	δ_u: cm	μ_T
R3 6D8	3838	6045	1·5750	1·46	3714	0·345	7·0259	14·05	1·9992
R3 6D12	5133	7417	1·4450	1·50	6624	0·584	14·2300	32·69	2·2973
R3 6C8	1450	4312	2·9738	1·46	3471	0·381	6·7193	14·20	2·1130
R3 6C12	1650	4398	2·6654	1·50	6015	0·640	11·1608	25·71	2·3038
R3 9D8	5578	9952	1·7841	1·46	4968	0·249	4·5044	16·44	3·6493
R3 9D12	7374	10864	1·4733	1·50	8557	0·431	8·7877	35·54	4·0439
R3 9C8	1916	8514	4·4436	1·46	4697	0·266	4·6515	6·72	1·4470
R3 9C12	2336	9050	3·8741	1·50	7792	0·470	9·5597	30·30	3·1695
R6 6D4	1160	4438	3·8258	1·35	1634	0·143	1·8625	3·49	1·8738
R6 6D8	1910	3250	1·7015	1·46	3547	0·363	4·3792	11·87	2·7105
R6 6D12	2478	3454	1·3938	1·50	6173	0·623	8·0935	25·66	3·1704
R6 6D16	2786	3465	1·2437	1·50	8713	0·983	14·232	41·31	2·9025
R6 6C4	566	4375	7·7296	1·35	1617	0·146	2·0415	3·80	1·8614
R6 6C8	742	3570	4·8113	1·46	3405	0·395	5·9420	13·60	2·2888
R6 6C12	832	3695	4·4411	1·50	5721	0·676	11·1279	25·12	2·2574
R6 6C16	914	4235	4·6334	1·50	8459	1·015	19·4083	56·81	2·9271
R6 9D4	1442	8178	5·6713	1·35	2108	0·111	1·6029	4·55	2·8385
R6 9D8	2780	7760	2·7913	1·46	4758	0·262	4·0320	7·26	1·8006
R6 9D12	3556	8618	2·4235	1·50	7971	0·459	8·4794	23·85	2·8126
R6 9D16	3872	9548	2·4660	1·50	10840	0·699	16·0817	48·69	3·0276
R6 9C4	736	7878	10·7038	1·35	2082	0·133	1·5354	3·49	2·2729
R6 9C8	998	7001	7·0150	1·46	4520	0·281	4·4045	8·34	1·8935
R6 9C12	1238	7398	5·9757	1·50	7456	0·492	8·8767	15·75	1·7743
R6 916	1302	8475	6·5092	1·50	10470	0·769	17·8824	36·65	2·0495

Table 5. Design base shear, over-strength factor and period-based ductility of model structures

performance requirements and the building has an acceptably low probability of collapse for maximum considered earthquake (MCE) ground motions. The spectral acceleration at which the model structure reaches a collapse state by a half of the seismic ground motions is defined as the median collapse capacity. Non-linear dynamic analyses are generally required to establish the median collapse capacity and the collapse margin ratio (CMR) for each of the analysis models. In Fema P695 (Fema, 2009), the ratio between the median collapse intensity ($\hat{S}_{CT}$) and the MCE intensity (S_{MT}) is defined as the CMR, which is the primary parameter used to characterise the collapse safety of the structure. Ground motion intensity is defined based on the median spectral intensity of the far-field record set, measured at the fundamental period of the structure. The Peer NGA database (Peer, 2006) provides 22 pairs of earthquake records for non-linear analysis of structures. The procedure for conducting non-linear response history analyses is based on the concept of incremental dynamic analysis (Vamvatsikos and Cornell, 2002), in which each ground motion is scaled to increasing intensities until the structure reaches a collapse point. Table 7-3 of Fema P695 provides acceptable values of adjusted collapse margin ratios ($ACMR_{10\%}$ and $ACMR_{20\%}$) based on total system collapse uncertainty and values of acceptable collapse probability, taken as 10% and 20% respectively.

Non-linear static analysis results

Non-linear static pushover analyses of all model structures were carried out along the transverse direction. The pushover curves of the structures designed with $R = 3$ are shown in Figure 4. The lateral load was determined proportional to the fundamental mode shape along this direction. Important points such as the design base shear, first yielding, maximum strength (V_{max}) and the strength corresponding to 80% of V_{max} are marked on the pushover curves. Table 5 lists the design and maximum base shears, over-strength factors and the period-based ductility factors obtained from the pushover curves. It was observed that the structures designed with $R = 3$ showed greater strength than those designed with $R = 6$. As the number of storeys increased, the strength and ductility of the model structures increased but the stiffness decreased. It can also be observed that stiffness starts to decrease when plastic hinges form in the first-storey columns. Plastic hinges then spread to the higher storey columns, followed by a decrease in strength.

Incremental dynamic analysis results

Incremental dynamic analyses of the model structures were carried out using the 22 pairs of scaled records to compute the CMRs of the model structures. A damping ratio of 5% was used for all vibration modes, which is generally used in non-linear

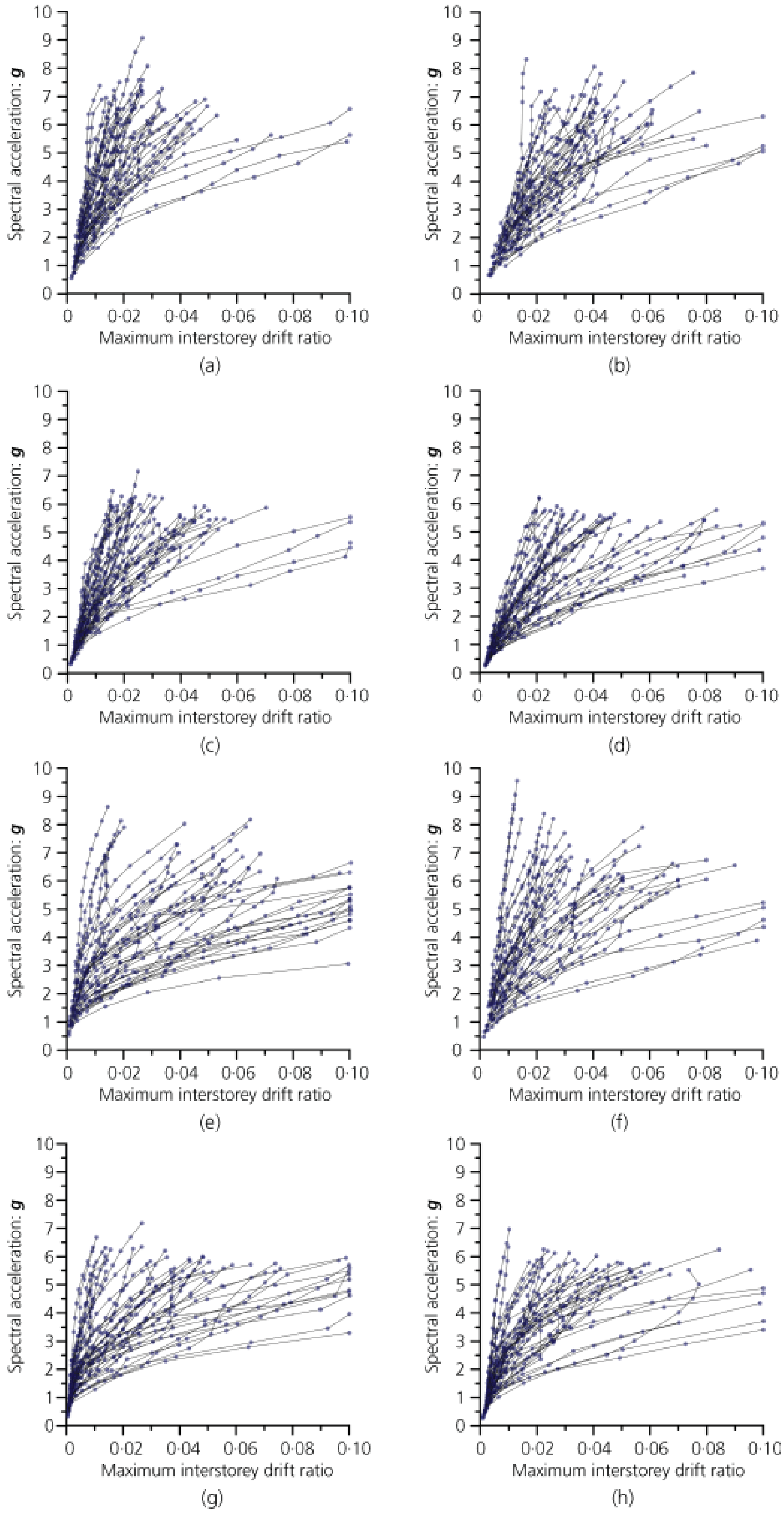

Figure 5. Incremental dynamic analysis of model structures with $R = 3$: (a) R3 6D8; (b) R3 6D12; (c) R3 6C8; (d) R3 6C12; (e) R3 9D8; (f) R3 9D12; (g) R3 9C8; (h) R3 9C12

	Model	$\hat{S}_{CT}$	CMR	SSF	ACMR	β_{tot}	$ACMR_{10\%}$	$ACMR_{20\%}$	Pass/Fail
PG1	R3 6D8	4·0574	2·7049	1·1316	3·0609	0·750		1·88	Pass
PG1	R3 6D12	4·3514	2·9009	1·1568	3·3554	0·750		1·88	Pass
Mean of PG1		4·2044	2·8000	1·1400	3·2100	0·750	2·61		Pass
PG2	R3 6C8	3·7806	5·0409	1·0635	5·3610	0·750		1·88	Pass
Mean of PG2		3·7806	5·0409	1·0635	5·3610	0·750	2·61		Pass
PG3	R3 6C12	3·2267	6·8844	1·0804	7·4379	0·750		1·88	Pass
Mean of PG3		3·2267	6·8844	1·0804	7·4379	0·750	2·61		Pass
PG4	R3 9D8	3·7500	2·5001	1·2359	3·0898	0·750		1·88	Pass
PG4	R3 9D12	4·0470	2·6983	1·2232	3·3005	0·750		1·88	Pass
Mean of PG4		3·8987	2·6000	1·2300	3·2000	0·750	2·61		Pass
PG5	R3 9C8	3·9529	5·2705	1·0341	5·4502	0·750		1·88	Pass
Mean of PG5		3·9529	5·2700	1·0341	5·4502	0·750	2·61		Pass
PG6	R3 9C12	4·0234	6·3034	1·0817	6·8184	0·750		1·88	Pass
Mean of PG6		4·0234	6·3034	1·0817	6·8184	0·750	2·61		Pass

Table 6. Evaluation of ACMRs of model structures designed with $R = 3$

	Model	$\hat{S}_{CT}$	CMR	SSF	ACMR	β_{tot}	$ACMR_{10\%}$	$ACMR_{20\%}$	Pass/Fail
PG1	R6 6D4	3·390	2·260	1·130	2·554	0·750		1·88	Pass
PG1	R6 6D8	3·569	2·379	1·165	2·771	0·750		1·88	Pass
Mean of PG1		3·479	2·319	1·147	2·662	0·750	2·61		Pass
PG2	R6 6D12	3·685	2·539	1·215	3·085	0·750		1·88	Pass
PG2	R6 6D16	3·078	3·352	1·248	4·183	0·750		1·88	Pass
Mean of PG2		3·3815	2·945	1·231	3·634	0·750	2·61		Pass
PG3	R6 6C4	3·148	4·198	1·052	4·418	0·750		1·88	Pass
PG3	R6 6C8	3·374	4·499	1·066	4·795	0·750		1·88	Pass
Mean of PG3		3·259	4·348	1·060	4·640	0·750	2·61		Pass
PG4	R6 6C12	2·887	6·544	1·083	7·088	0·750		1·88	Pass
PG4	R6 6C16	2·256	7·671	1·139	8·737	0·750		1·88	Pass
Mean of PG4		2·572	7·108	1·111	7·913	0·750	2·61		Pass
PG5	R6 9D4	3·269	2·179	1·165	2·538	0·750		1·88	Pass
PG5	R6 9D8	3·309	2·206	1·115	2·460	0·750		1·88	Pass
PG5	R6 9D12	3·321	2·214	1·170	2·590	0·750		1·88	Pass
Mean of PG5		3·299	2·199	1·150	2·529	0·750	2·61		FAIL
PG6	R6 9D16	3·036	2·362	1·210	2·858	0·750		1·88	Pass
Mean of PG6		3·036	2·362	1·210	2·858	0·750	2·61		Pass
PG7	R6 9C4	3·195	4·260	1·065	4·537	0·750		1·88	Pass
PG7	R6 9C8	3·470	4·627	1·056	4·886	0·750		1·88	Pass
Mean of PG7		3·333	4·443	1·061	4·712	0·750	2·61		Pass
PG8	R6 9C12	3·576	5·841	1·051	6·139	0·750		1·88	Pass
PG8	R6 9C16	2·788	7·157	1·080	7·729	0·750		1·88	Pass
Mean of PG8		3·182	6·499	1·065	6·934	0·750	2·61		Pass

Table 7. Evaluation of ACMRs of model structures designed with $R = 6$

dynamic analysis of structures subjected to inelastic deformation (Chopra, 2007). The incremental dynamic analysis results for spectral acceleration versus maximum interstorey drift ratio of the model structures designed with $R = 3$ are presented in Figure 5. The median collapse intensity or the spectral acceleration ($\hat{S}_{CT}$) at which dynamic instability of each model structure was initiated by the 22nd earthquake record was determined from the incremental dynamic analysis curves. The state of dynamic instability was defined as the point at which the stiffness of the structure decreased to 20% of the initial stiffness (Vamvatsikos and Cornell, 2002). It was observed that, at the state of dynamic instability, interstorey drifts of most of the model structures reached around 2% of the storey height. Tables 6 and 7 show the median collapse intensities of the model structures designed with R factors of 3 and 6 respectively.

The CMR, which is the primary parameter used to characterise the collapse safety of a structure, was obtained from the ratio of the median collapse intensity $\hat{S}_{CT}$ and the MCE intensity S_{MT}. The SSFs of the model structures were obtained from table 7-1 of Fema P695 (Fema, 2009) using the natural periods and period-based ductility coefficients presented in Table 5. The SSFs obtained in this way were multiplied by the CMR to compute the ACMR values, which are shown in Tables 6 and 7. The total system collapse uncertainty (β_{tot}) of the model structures was determined based on the assumption that the qualities of design requirements were 'fair' and model quality was 'good'. As sufficient test data have not yet been provided regarding the seismic capacity of staggered wall structures, the quality of the test data was considered to be 'poor'. Using table 7-2b of Fema P695, β_{tot} was obtained as 0·75. From table 7-3 of Fema P695, the acceptable values of ACMR corresponding to a collapse probability of 10% ($ACMR_{10\%}$) and 20% ($ACMR_{20\%}$) were found to be 2·61 and 1·88 respectively for $\beta_{tot} = 0{\cdot}75$. In the model structures designed with $R = 3$ and SDC D_{max} (PG1 and PG4), ACMR ranged from 3·06 to 3·36 and satisfied the acceptable value of $ACMR_{20\%}$. The mean value of each performance group satisfied the acceptable value of $ACMR_{10\%}$. The performance groups corresponding to SDC C_{max} (PG2, PG3, PG5 and PG6) also satisfied $ACMR_{10\%}$ and $ACMR_{20\%}$. This implies that a response modification factor of 3 may be used for seismic design of the model structures. However, the collapse margin for the structures designed with $R = 3$ was two to four times larger than the given acceptable values for $ACMR_{10\%}$ and $ACMR_{20\%}$. Table 7 shows that the ACMR of the structures designed with $R = 6$ ranged from 2·46 to 8·74. Even though the ACMRs of the model structures exceeded the acceptable value specified for $ACMR_{20\%}$, the mean value of performance group PG5 was less than the acceptable value $ACMR_{10\%}$ and was thus considered to be inadequate.

Fragility analysis results

Fragility curves show the probability of a system reaching a limit state as a function of a seismic intensity measure. In this study, pseudo spectral acceleration was used as the seismic intensity measure, and the seismic fragility was obtained from the results of incremental dynamic analysis. Fragility was described by the conditional probability that the structural capacity C fails to resist the structural demand D. It is generally modelled as a log-normal cumulative density function (Vamvatsikos and Cornell, 2002) given by

$$P(D < C) = 1 - \Phi\left[\frac{\ln(\hat{C}/D)}{\beta_c}\right] \quad (3)$$

in which $\Phi[\cdot]$ is the standard normal probability integral, $\hat{C}$ is the median structural capacity associated with a limit state, D is the median structural demand and β_c is system collapse uncertainty. The log-normal collapse fragility is defined by the median collapse intensity $\hat{S}_{CT}$ and the standard deviation of the natural logarithm. The median collapse capacity corresponds to a 50% probability of collapse.

Figure 6 shows the fragility curve for the model R3 9D8. The horizontal axis in Figure 6 represents the seismic intensity corresponding to a certain level of collapse probability. If it is normalised by the MCE intensity, it represents the ratio between the earthquake intensity that causes collapse and the MCE intensity for which the structure has been designed. The collapse ratio at the median point is termed the CMR. Haselton and Baker (2006) demonstrated the importance of considering the unique spectral shape of extreme ground motions when evaluating collapse, and Fema P695 (Fema, 2009) requires that the CMR is multiplied by the SSF to shift the fragility curve to the right. The new median point, the ACMR, anchors the shifted fragility curve.

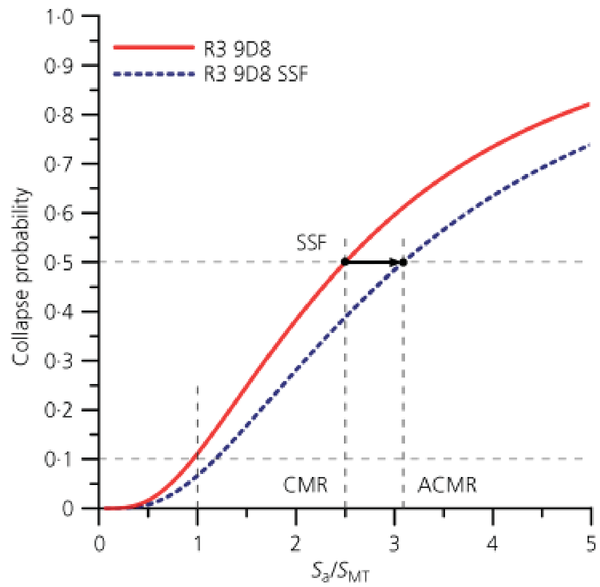

Figure 6. Modified fragility curve considering the SSF

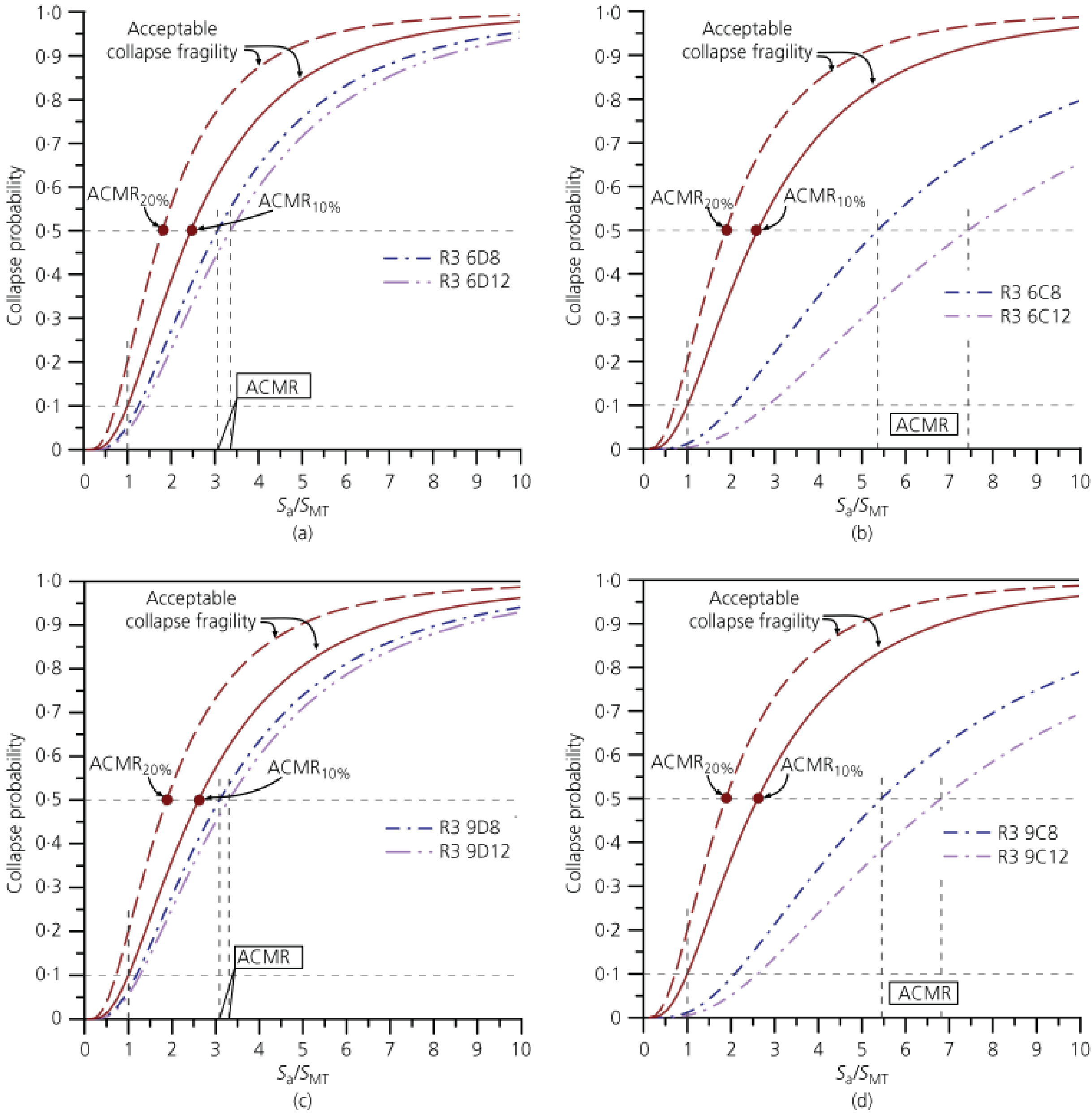

Figure 7. Fragility curves of model structures designed with $R = 3$: (a) PG1; (b) PG2, PG3; (c) PG4; (d) PG5, PG6

Figure 6 illustrates the significant reduction in the probability of collapse at the MCE after consideration of the SSF.

Figures 7 and 8 depict the fragility curves of the model structures designed with R factors of 3 and 6 respectively. The acceptable collapse fragility and the acceptable values of the ACMR provided in Fema P695 are also indicated in the figures. It is required that the average CMR for each performance group is greater than $ACMR_{10\%}$ and that the individual values of ACMR for each index archetype within a performance group exceed $ACMR_{20\%}$. These acceptance criteria imply that the probability of collapse for MCE ground motions is approximately 10% or less, on average across a performance group, and the probability of collapse for MCE ground motions is approximately 20% or less for each index archetype within a performance group. Figure 7 shows that the collapse probabilities of the model structures designed with $R = 3$ are smaller than the acceptable collapse probability, and the ACMR is larger than the acceptable values of $ACMR_{10\%}$ and $ACMR_{20\%}$. In particular, the ACMR values of the structures corresponding to SDC C_{max} are 1·8–2·2 times those of the structures corresponding to SDC D_{max}. Similar results were obtained in the structures designed with $R = 6$, except that the

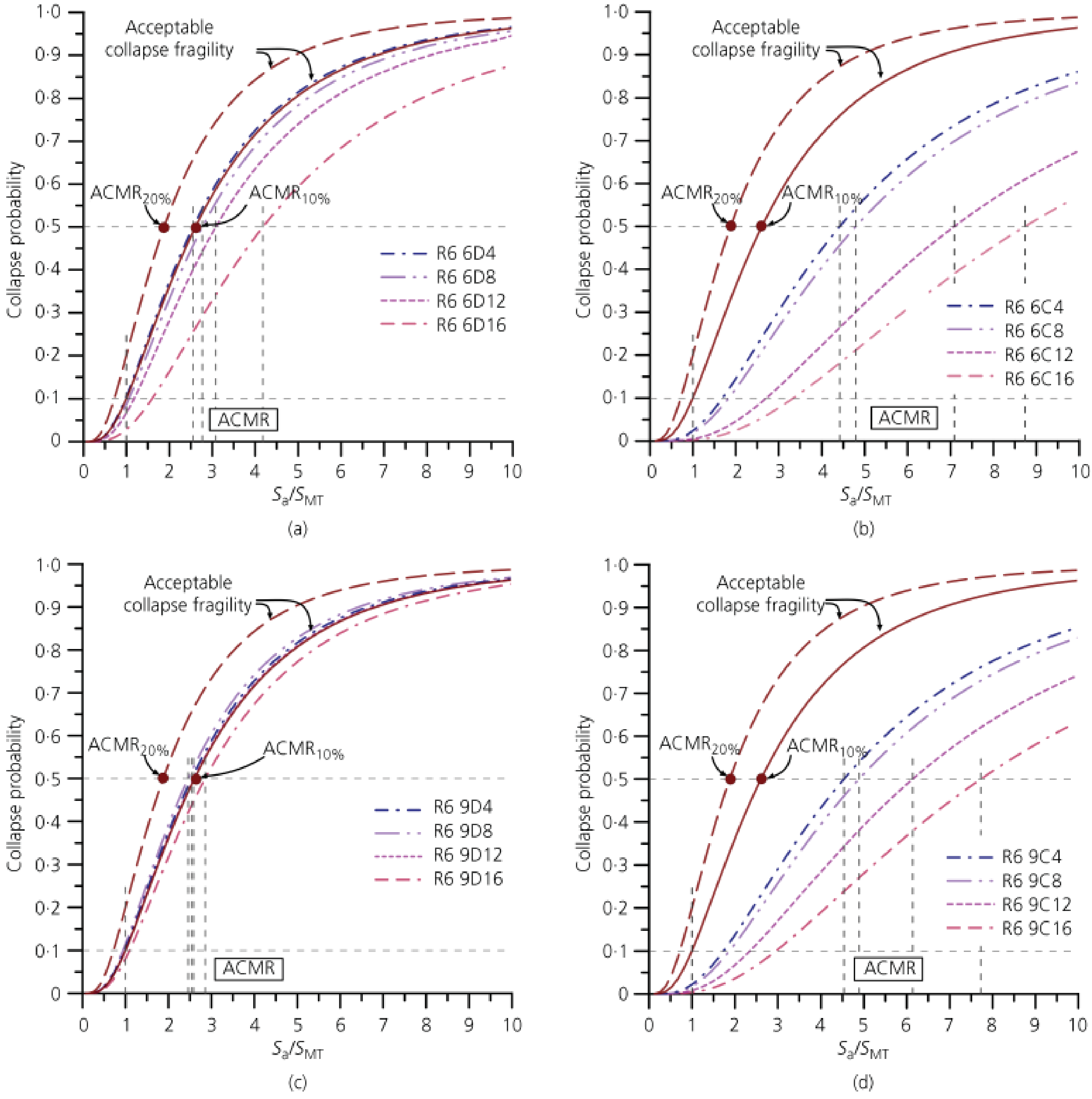

Figure 8. Fragility curves of model structures designed with $R = 6$: (a) PG1, PG2; (b) PG3, PG4; (c) PG5, PG6; (d) PG7, PG8

ACMR of some structures belonging to SDC D_{max} were less than $ACMR_{10\%}$, as shown in Figure 8.

Figure 9 compares the fragility curves of the structures with 9 m staggered walls designed with R factors of 3 and 6. The collapse probabilities of the structures designed with $R = 6$ are larger than those of the structures designed with $R = 3$. It can also be seen that the ACMR of the structures tends to increase as the number of storeys increases, except for the four-storey structure R6 9D4: the column sizes of R6 9D4 were determined with a minimum size requirement, and consequently designed with member strength ratios smaller than those of the other structures.

Figure 10 shows the mean fragility curves of the model structures R6 PG5 and R3 PG4 and the acceptable collapse fragility curve. It can be seen that the mean collapse fragility of model R3 PG4 is smaller than the acceptable fragility. However, the mean fragility curve of model R6 PG5 exceeds the acceptable fragility curve and the mean ACMR exceeds $ACMR_{10\%}$. Therefore, some of the model structures designed with $R = 6$ fail to satisfy the

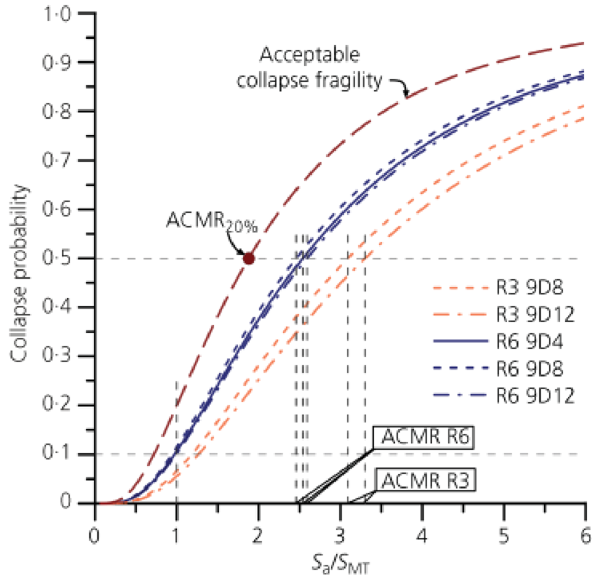

Figure 9. Comparison of fragility curves of model structures designed with $R = 3$ and $R = 6$

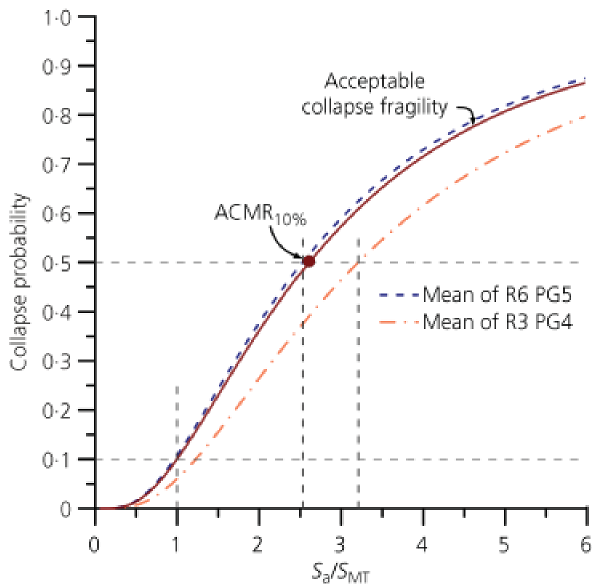

Figure 10. Mean fragility curves of model structures R6 PG5 and R3 PG4

acceptance criterion specified in Fema P695 (Fema, 2009). This implies that the R factor of 6 is not adequate for staggered wall structures.

ASCE 7-10 (ASCE, 2010) specifies that the response modification factors for ordinary and special RC shear wall structures in the category of 'bearing wall systems' are 4 and 5 respectively, and those in 'building frame systems' are 5 and 6 respectively. As the results of this study showed that $R = 6$ is slightly high for staggered wall systems, R factors of 4 and 5 seem to be appropriate for staggered wall system structures designed without and with seismic detailing respectively. However, considering the fact that more experimental verifications for the seismic performance of staggered wall structures are still required, slightly smaller values may be acceptable as R factors for conservative design.

Conclusions

This study investigated the response modification factor for RC staggered wall structures based on the Fema P695 (Fema, 2009) approach. In total, 24 model structures were designed as per ASCE 7-10 (ASCE, 2010) using two different response modification factors, and were categorised into 14 performance groups. Incremental dynamic analyses were carried out using 44 earthquake records, and the results were used to obtain fragility curves. The validity of the response modification factor (R) was investigated by comparing the adjusted collapse margin ratios with acceptable values according to Fema P695.

The results of the analysis showed that structures designed with lower intensity seismic load (SDC C_{max}) have a lower collapse probability than structures designed with a higher intensity seismic load (SDC D_{max}). It was also found that the model structures designed with $R = 3$ satisfied the acceptance criteria specified in Fema P695, but some of the model structures designed with $R = 6$ failed to satisfy the acceptance criteria.

ASCE 7-10 (ASCE, 2010) suggests response modification factors for shear wall structures varying from 4 to 6 depending on the seismic detailing and the category of the seismic load resisting system. Based on the results of this study, and comparison with the R factors specified for shear wall structures in the design code, R factors of 4 and 5 are respectively recommended for staggered wall system structures designed without and with seismic detailing.

Acknowledgements

This research was financially supported by the Samsung Research Fund of Sungkyunkwan University.

REFERENCES

ACI (American Concrete Institute) (2014) ACI 318: Building code requirements for structural concrete (318-14) and commentary. ACI, Farmington Hills, MI, USA.

ASCE (2010) ASCE 7-10: Minimum design loads for buildings and other structures. ASCE, Reston, VA, USA.

Chopra AK (2007) *Dynamics of Structures*, 3rd edn. Prentice-Hall, Upper Saddle River, NJ, USA.

CSI (Computers and Structures, Inc.) (2006) *Perform-3D. Nonlinear analysis and Performance Assessment for 3D Structures – User Guide*. CSI, Berkeley, CA, USA.

Fema (Federal Emergency Management Agency) (2003) Fema 450: NEHRP Recommended Provisions for Seismic

Regulations and Other Structures. Fema, Washington, DC, USA.

Fema (2009) Fema P695: Quantification of building seismic performance factors. Fema, Washington, DC, USA.

Fintel M (1968) Staggered transverse wall beams for multistory concrete buildings. *ACI Journal* **65(5)**: 366–78.

Haselton CB and Baker JW (2006) Ground motion intensity measures for collapse capacity prediction: Choice of optimal spectral period and effect of spectral shape. *Proceedings of 8th National Conference on Earthquake Engineering, San Francisco, CA, USA*.

ICC (International Code Council) (2009) *International Building Code*. ICC, Falls Church, VA, USA.

Kim J and Jun Y (2011) Seismic performance evaluation of partially staggered wall apartment buildings. *Magazine of Concrete Research* **63(12)**: 927–939, http://dx.doi.org/10.1680/macr.10.00140.

Kim J and Lee M (2014) Fundamental period formulae for RC staggered wall buildings. *Magazine of Concrete Research* **66(7)**: 325–338, http://dx.doi.org/10.1680/macr.13.00253.

Lee J and Kim J (2013) Seismic performance evaluation of staggered wall structures using Fema P695 procedure. *Magazine of Concrete Research* **65(17)**: 1023–1033, http://dx.doi.org/10.1680/macr.12.00237.

Mee AL, Jordaan IJ and Ward MA (1975) Dynamic response of a staggered wall–beam structure. *Earthquake Engineering and Structural Dynamics* **3(4)**: 353–364.

Paulay T and Priestley MJN (1992) *Seismic Design of Reinforced Concrete and Masonry Building*. Wiley, Chichester, UK.

Peer (Pacific Earthquake Engineering Research Center) (2006) *Peer NGA Database*. Peer, University of California, Berkeley, CA, USA. See http://peer.berkeley.edu/nga (accessed 27/04/2015).

Peer (2011) *Case Studies of the Seismic Performance of Tall Buildings Designed by Alternative Means*. Peer, University of California, Berkeley, CA, USA, Peer report 2011/05

Vamvatsikos D and Cornell CA (2002) Incremental dynamic analysis. *Earthquake Engineering and Structural Dynamics* **31(3)**: 491–514.